


# Quantum electrodynamic effects on counter-streaming instabilities in the whole $\mathbf{k}$ space

Antoine Bret \*

*ETSI Industriales, Universidad de Castilla-La Mancha, 13071 Ciudad Real, Spain*

*and Instituto de Investigaciones Energéticas y Aplicaciones Industriales, Campus Universitario de Ciudad Real, 13071 Ciudad Real, Spain*



(Received 28 October 2021; accepted 1 January 2022; published 12 January 2022)

In a recent work [Bret, *EPL* **135**, 35001 (2021)], quantum electrodynamic (QED) effects were evaluated for the two-stream instability. It pertains to the growth of perturbations with a wave vector oriented along the flow in a collisionless counter-streaming system. Here, the analysis is extended to every possible orientation of the wave vector. The previous result for the two-stream instability is recovered, and it is proved that, even within the framework of a three-dimensional (3D) analysis, this instability remains fundamentally 1D even when accounting for QED effects. The filamentation instability, found for wave vectors normal to the flow, is weakly affected by QED corrections. As in the classical case, its growth rate saturates at large  $k_{\perp}$ . The saturation value is found independent of QED corrections. Also, the smallest unstable  $k_{\perp}$  is independent of QED corrections. Surprisingly, unstable modes found for oblique wave vectors do *not* follow the same pattern. For some, QED corrections do reduce the growth rate. But, for others, the same corrections increase the growth rate instead. The possibility for QED effects to play a role in unmagnetized systems is evaluated. Pair production resulting from  $\gamma$  emission by particles oscillating in the exponentially growing fields is not accounted for.

DOI: [10.1103/PhysRevE.105.015205](https://doi.org/10.1103/PhysRevE.105.015205)

## I. INTRODUCTION

Counter-streaming instabilities have been a central topic in plasma physics for nearly one century [1,2]. Extreme plasma physics, on the other hand, has been rising during the past years [3,4]. It has to do with quantum electrodynamic (QED) effects that could appear in plasmas immersed in extreme electromagnetic fields. This new field of research is spurred by the advent of high-power lasers with which such effects could be observed [5,6]. Also involved are high energy astrophysics settings, like magnetars or pulsars, where magnetic fields of the order of the critical Schwinger field  $B_{cr} = m^2 c^3 / q \hbar = 4.4 \times 10^{13}$  G, or even greater, are present [7,8].

In neutron stars or magnetars, particle beams flow along the field lines from one foot of the lines to the other. It is yet unclear how they are stopped when hitting the surface. There, counter-streaming instabilities could play a role in the dissipation of the kinetic energy [9]. Such instabilities have also been invoked in the context of pulsar emissions [10–12].

With fields  $B_0$  of the order of  $10^{12}$  G for neutron stars, the ratio  $B_0/B_{cr}$  reaches 0.02 so that corrections described here are necessary. As for magnetars, the ratio  $B_0/B_{cr}$  reaches 2 to 22 so that the present corrections are but preliminaries for even greater ones since the present treatment assumes  $B_0/B_{cr} \ll 1$ .

In the context of long  $\gamma$ -ray bursts, some models propose a protomagnetar as central engine [13–15]. As the jet it produces makes its way through the remainder of the progenitor star, counter-streaming instabilities in a highly magnetized environment should be excited, especially in the inner part of

the jet. Here, the field of the protomagnetar would also render necessary QED corrections.

It seems therefore natural to investigate QED effects on counter-streaming instabilities as they could be triggered in various high field environments. Recently, QED effects were studied for the two-stream instability (TSI) in the presence of a guiding magnetic field  $B_0$  [16]. It was found that, for  $B_0 \ll B_{cr}$ , the growth rate is scaled down by a factor  $\sqrt{1 + \xi}$  with

$$\xi = \frac{\alpha}{9\pi} \left( \frac{B_0}{B_{cr}} \right)^2, \quad (1)$$

where  $\alpha \sim 1/137$  is the fine structure constant.

Still, it has been known for a long time that the TSI is not the only instability triggered in collisionless counter-streaming systems [17–19]. While the TSI amplifies perturbations  $\propto \exp(i\mathbf{k} \cdot \mathbf{r} - i\omega t)$  with  $\mathbf{k}$  parallel to the flow, perturbations with  $\mathbf{k}$  normal and even oblique to the flow can also grow as the filamentation instability (FI) and the oblique instability, respectively. Depending on the parameters of the problem, various instabilities can dominate the unstable spectrum, and their hierarchy has been worked out for several kinds of systems [20–25].

The goal of this article is to extend the study of QED effects on the TSI to every possible perturbation. We consider the simple system pictured on Fig. 1. Two counter-streaming cold electron beams of identical density  $n_0$  and opposed velocities  $\pm \mathbf{v}_0$  stream along the  $z$  axis. “Cold” here means that the thermal velocity spread  $\Delta v$  in each beam satisfies  $\Delta v \ll v_0$ . A background of fixed ions ensures charge neutrality. An external magnetic field  $\mathbf{B}_0$  is aligned with the flow. The system is therefore charge and current neutral at equilibrium, with no force acting on it since  $\mathbf{v}_0 \times \mathbf{B}_0 = \mathbf{0}$ .

\*antoineclaude.bret@uclm.es

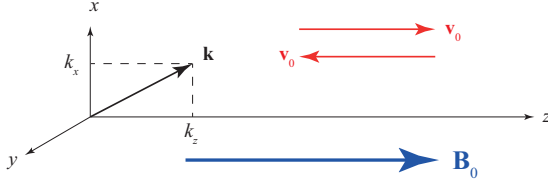


FIG. 1. System considered.

Perturbations with wave vector  $\mathbf{k}$  are applied. Since the system has cylindrical symmetry around  $z$ , we can choose the  $x, y$  directions such that  $k = (k_x, 0, k_z)$  without loss of generality.

In Sec. II we briefly recall the structure of the classical calculation in order to clearly see where QED corrections come into play. Then, in Sec. III, QED corrections are worked out.

## II. CLASSICAL CALCULATION

Since the beams are assumed cold, a two-fluids model can be implemented. We write the conservation equations for matter and momentum for the two beams,

$$\frac{\partial n_i}{\partial t} + \nabla \cdot (n_i \mathbf{v}_i) = 0, \quad (2)$$

$$\frac{\partial \mathbf{p}_i}{\partial t} + (\mathbf{v}_i \cdot \nabla) \mathbf{p}_i = q \left( \mathbf{E} + \frac{\mathbf{v}_i \times \mathbf{B}}{c} \right), \quad (3)$$

where the momentum  $p_i$  reads  $p_i = \gamma_i m v_i$  with  $\gamma_i = (1 - v_i^2/c^2)^{-1/2}$ ,  $m$  the electron mass, and  $q$  its charge. We also write the Maxwell's equations involved in the calculation,

$$\nabla \times \mathbf{E} = -\frac{1}{c} \frac{\partial \mathbf{B}}{\partial t}, \quad (4)$$

$$\nabla \times \mathbf{B} = \frac{1}{c} \frac{\partial \mathbf{E}}{\partial t} + \frac{4\pi}{c} \mathbf{J}. \quad (5)$$

The full calculation can be found in Refs. [22,26]. It goes as follows. Assume first order perturbations  $\propto \exp(i\mathbf{k} \cdot \mathbf{r} - i\omega t)$  of every quantity and linearize Eqs. (2)–(5). Equations (2) and (3) give the first order density perturbation  $n_{1i}$ . Then Eq. (3) gives the first order velocity perturbation  $\mathbf{v}_{1i}$  in terms of  $\mathbf{E}_1$ ,  $\mathbf{B}_1$ , and  $\mathbf{B}_0$ . Finally, Eq. (4) gives  $\mathbf{B}_1 = (c/\omega)\mathbf{k} \times \mathbf{E}_1$ .

The classical current can then be computed as

$$\mathbf{J}_{\text{class}}(\mathbf{E}_1) = q \underbrace{\sum_i n_0 \mathbf{v}_0}_{=0} + q \sum_i n_{0i} \mathbf{v}_{1i} + n_{1i} \mathbf{v}_{0i}. \quad (6)$$

Finally, Eq. (5) is used to obtain

$$\mathbf{k} \times (\mathbf{k} \times \mathbf{E}_1) + \frac{\omega^2}{c^2} \left( \mathbf{E}_1 + \frac{4i\pi}{\omega} \mathbf{J}_{\text{class}}(\mathbf{E}_1) \right) = 0, \quad (7)$$

that is, a tensorial equation of the form  $\mathfrak{T}(\mathbf{E}_1) = \mathbf{0}$ . The dispersion equation then comes through  $\det \mathfrak{T} = 0$ . Note that, when considering the TSI, the dispersion equation can be obtained from the scalar Poisson equation since the problem is one dimensional (1D). Here, we need to use the vectorial Maxwell-Faraday equation for the current since the problem is 3D.

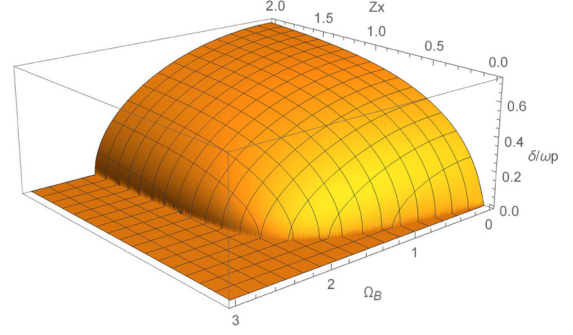


FIG. 2. Growth rate of the classical FI in terms of the field amplitude  $\Omega_B$  and the wave vector  $Z_x$ . The growth rate saturates at large  $Z_x$  and the instability is stabilized for  $\Omega_B > \beta_0 \sqrt{2\gamma_0}$ .

Although without major technical difficulties, calculations are lengthy. They can be performed with the *Mathematica* Notebook described in Ref. [27] in terms of the dimensionless variables,

$$x = \frac{\omega}{\omega_p}, \quad \mathbf{Z} = \frac{\mathbf{k} v_0}{\omega_p}, \quad \beta_0 = \frac{v_0}{c}, \quad \gamma_0 = \frac{1}{\sqrt{1 - \beta_0^2}},$$

$$\Omega_B = \frac{\omega_B}{\omega_p}, \quad \omega_B = \frac{|q| B_0}{mc}, \quad (8)$$

with

$$\omega_p^2 = \frac{4\pi n_0 q^2}{m}. \quad (9)$$

The *Mathematica* Notebook used to compute the dispersion equation is provided as Supplemental Material [28].

The salient and known features of the classical case are as follows.

(i) For  $Z_x = 0$ , that is  $\mathbf{k}$  parallel to the flow, the TSI is left unchanged by the field since it has particles oscillating along the field, hence canceling the Lorentz force.

(ii) For  $Z_z = 0$ , that is  $\mathbf{k}$  normal to the flow, the growth rate  $\delta$  of the FI is pictured on Fig. 2 in terms of  $Z_x$  and  $\Omega_B$ . For large  $Z_x$ , the growth rate saturates at [26]

$$\delta(Z_x = \infty) = \frac{\sqrt{2\beta_0^2 \gamma_0 - \Omega_B^2}}{\gamma_0}. \quad (10)$$

The most direct and interesting consequence of this equation is that FI is quenched beyond the critical value,

$$\Omega_B > \beta_0 \sqrt{2\gamma_0} \equiv \Omega_{Bc}. \quad (11)$$

The field also stabilizes the small wavelengths fulfilling (see details in Sec. III B)

$$Z_x < \frac{\sqrt{2}}{\gamma_0^{3/2}} \frac{\beta_0 \Omega_B}{\sqrt{2\beta^2 \gamma_0 - \Omega_B^2}}. \quad (12)$$

(iii) For both  $Z_x, Z_z \neq 0$ , Fig. 3 pictures a typical growth rate map in terms of  $Z_x$  and  $Z_z$ . The amplitude of the field  $\Omega_B = 3 > \beta_0 \sqrt{2\gamma_0} \sim 2.3$  is such that the FI is stabilized. The TSI is left unchanged with respect to the field-free case. The dominant unstable modes are now oblique. We refer the reader

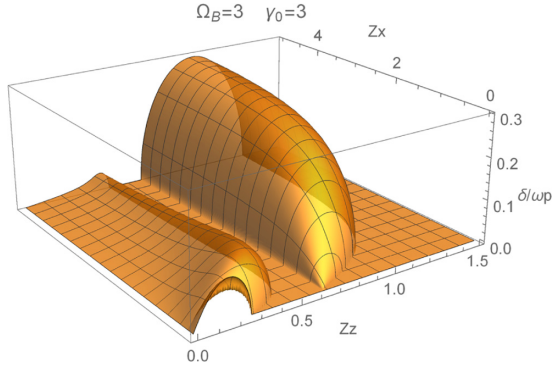


FIG. 3. Classical growth rate  $\delta$  in terms of  $Z_x$  and  $Z_z$ . The amplitude of the field  $\Omega_B = 3 > \beta_0 \sqrt{2\gamma_0} \sim 2.3$  is such that the filamentation instability is stabilized. The TSI is left unchanged with respect to the field-free case. The dominant unstable modes are now oblique.

to Ref. [26] for the analysis of the unstable upper-hybrid-like modes with  $Z_z \neq 0$  and  $Z_x \gg 1$ .

### III. QED CALCULATION

QED corrections only modify the expression (6) for the current.<sup>1</sup> It now reads

$$\mathbf{J} = \mathbf{J}_{\text{class}} + \mathbf{J}_{\text{vac}}, \quad (13)$$

where  $\mathbf{J}_{\text{class}}$  is the classical result and

$$\mathbf{J}_{\text{vac}} = -\frac{1}{180\pi^2} \frac{\alpha}{c^2 B_{cr}^2} \left( \nabla \times \mathbf{M} - \frac{\partial \mathbf{P}}{\partial t} \right), \quad (14)$$

where

$$\mathbf{M} = 2(E^2 - c^2 B^2) c \mathbf{B} - 7c(\mathbf{E} \cdot \mathbf{B}) \mathbf{E}, \quad (15)$$

$$\mathbf{P} = 2(E^2 - c^2 B^2) \mathbf{E} + 7c^2(\mathbf{E} \cdot \mathbf{B}) \mathbf{B}. \quad (16)$$

Since the  $\nabla \times$  and the  $\partial_t$  operators are linear, we can linearize  $\mathbf{M}$  and  $\mathbf{P}$  first, before applying these operators to obtain the linearized version of Eq. (14). The linearization of Eqs. (15) and (16) gives

$$\mathbf{M} = -\begin{pmatrix} 0 \\ 0 \\ 2B_0^3 c^3 + \frac{4B_0^2 c^4 E_{1y} k_x}{\omega} \end{pmatrix} + O(E_1^2), \quad (17)$$

$$\mathbf{P} = \begin{pmatrix} -2B_0^2 c^2 E_{1x} \\ -2B_0^2 c^2 E_{1y} \\ 5B_0^2 c^2 E_{1z} \end{pmatrix} + O(E_1^2). \quad (18)$$

Since  $E_{1x,y,z} \propto \exp(i\mathbf{k} \cdot \mathbf{r} - i\omega t)$  we find from Eq. (14) the QED correction to the first order current,

$$\mathbf{J}_{1,\text{vac}} = i\omega \frac{\xi}{20\pi} \left( \frac{B_0}{B_{cr}} \right)^2 \begin{pmatrix} 2E_{1x} \\ 2\left(1 - 2\frac{c^2 k_x^2}{\omega^2}\right) E_{1y} \\ -5E_{1z} \end{pmatrix}, \quad (19)$$

where  $\xi$  is the dimensionless parameter defined by Eq. (1).

All the steps described for the classical case are therefore identical, except that we now need to add  $\mathbf{J}_{1,\text{vac}}$  to the current equation (6). The dispersion equation is eventually still of the form  $\det \mathfrak{T} = 0$  with now

$$\mathfrak{T} = \mathfrak{T}_{\text{class}} + \xi \mathfrak{T}_{\text{QED}}, \quad (20)$$

with

$$\mathfrak{T}_{\text{QED}} = \begin{pmatrix} -\frac{2}{5} & 0 & 0 \\ 0 & \frac{2}{5} \left( \frac{2Z_x^2}{x^2 \beta_0^2} - 1 \right) & 0 \\ 0 & 0 & 1 \end{pmatrix}, \quad (21)$$

so that the correction for all  $\mathbf{k}$ 's is of order  $\xi$  and diagonal only.

Note that, for all practical purposes,  $\xi$  is an extremely small parameter since  $B_0 \ll B_{cr}$  is required to write Eqs. (13) and (14) on the one hand (see [30] or [31], p. 32), while  $\alpha \sim 1/137$  on the other hand. For example, with  $B_0/B_{cr} = 0.1$ , Eq. (1) gives  $\xi = 2.5 \times 10^{-6}$ . Even  $\xi = 0.1$  requires  $B_0 = 19B_{cr}$ , which is far out of range of the present theory.

Computing the dispersion equation is performed using a *Mathematica* Notebook very similar to the one used for the classical case. The only difference is that the QED-corrected first order current (19) is added to Eq. (5) of Ref. [27].

Since the dispersion equation reads  $\det \mathfrak{T} = 0$ , where  $\mathfrak{T}$  is now given by Eq. (20), an alternative to the forthcoming calculations would be to write

$$\mathfrak{T}_{\text{class}} + \xi \mathfrak{T}_{\text{QED}} = \mathfrak{T}_{\text{class}} (I + \xi \mathfrak{T}_{\text{class}}^{-1} \mathfrak{T}_{\text{QED}}), \quad (22)$$

so that

$$\begin{aligned} \det \mathfrak{T} &= \det \mathfrak{T}_{\text{class}} \times \det (I + \xi \mathfrak{T}_{\text{class}}^{-1} \mathfrak{T}_{\text{QED}}) \\ &= \det \mathfrak{T}_{\text{class}} \times \{1 + \xi \text{tr}(\mathfrak{T}_{\text{class}}^{-1} \mathfrak{T}_{\text{QED}}) + O(\xi^2)\}, \end{aligned} \quad (23)$$

where  $\text{tr} \mathfrak{M}$  is the trace of the matrix  $\mathfrak{M}$  and Jacoby's formula has been used to expand the determinant  $\det(I + \xi \mathfrak{T}_{\text{class}}^{-1} \mathfrak{T}_{\text{QED}})$ . The dispersion equation would then read, at first order in  $\xi$ ,

$$\det \mathfrak{T} = 0 \Rightarrow 1 + \xi \text{tr}(\mathfrak{T}_{\text{class}}^{-1} \mathfrak{T}_{\text{QED}}) = 0. \quad (24)$$

However, since the dispersion equation is to be solved for  $x$  and not  $\xi$ , computations are not simpler than the ones explained from now. We now review the consequences of the QED corrections on the various instabilities involved in the system.

#### A. Two-stream instability (TSI)

Since the TSI pertains to wave vectors aligned with the flow, we set  $Z_x = 0$  in Eq. (20). The result is a tensor of the form

$$\mathfrak{T} = \begin{pmatrix} T_{11} & T_{12} & 0 \\ T_{12}^* & T_{22} & 0 \\ 0 & 0 & T_{33} \end{pmatrix}, \quad (25)$$

where  $z^*$  is the complex conjugate of  $z$ . The dispersion equation then reads

$$T_{33}(T_{11}T_{22} - T_{12}^*T_{12}) = 0. \quad (26)$$

The second factor can be further factorized, but the subfactors still are fourth degree polynomials in  $x$ , with both even and

<sup>1</sup>See, for example, Eqs. (1)–(8) of Ref. [29].

odd powers of  $x$ . They are therefore difficult to deal with analytically. Yet, a numerical exploration shows that, at least in the regime  $B_0 \ll B_{cr}$ , they do not yield unstable modes. The instability comes therefore from  $T_{33} = 0$ , which is the usual dispersion equation for the TSI. In the present case with QED corrections, the equation derived in Ref. [16] is recovered, namely,

$$1 + \xi - \frac{1}{\gamma_0^3(x - Z_z)^2} - \frac{1}{\gamma_0^3(x + Z_z)^2} = 0. \quad (27)$$

We therefore here extend the results of Ref. [16]: even when considering a full 3D system, the QED-corrected TSI is still 1D like.

### B. Filamentation instability (FI)

The FI pertains to wave vectors normal to the flow. We therefore set  $Z_z = 0$  in Eq. (20). A tensor of the form (25) is obtained again, yielding a dispersion equation of the form (26).

In the classical case, the tensor element  $T_{33}$  is the one which yields the instability. Here it reads

$$T_{33} = 1 + \xi - \frac{1}{x^2} \left( \frac{2}{\gamma_0^3} + \frac{Z_x^2}{\beta_0^2} + \frac{1}{\gamma_0} \frac{2Z_x^2}{x^2 - \Omega_B^2/\gamma_0^2} \right). \quad (28)$$

In the case of the TSI, Eq. (27) makes it possible to rescale  $x$  and  $Z_z$  (or  $\gamma_0$ ) and formally come back to the classical TSI dispersion equation [16]. Such a procedure is not possible here. Still, some analytical conclusions can be reached.

For large  $Z_x$ , Eq. (28) gives the dispersion equation,

$$\begin{aligned} -\frac{1}{x^2} \left( \frac{Z_x^2}{\beta_0^2} \right) - \frac{2\gamma_0 Z_x^2}{\gamma_0^2 x^4 - x^2 \Omega_B^2} &= 0 \\ \Rightarrow \frac{1}{\beta_0^2} + \frac{2\gamma_0}{\gamma_0^2 x^2 - \Omega_B^2} &= 0 \\ \Rightarrow x^2 &= \frac{\Omega_B^2 - 2\beta_0^2 \gamma_0}{\gamma_0^2}. \end{aligned} \quad (29)$$

This corresponds exactly to the classical growth rate (10). Therefore, QED effects do not affect the saturation value of the FI, nor the value of the magnetic field required to cancel it.

Regarding the stabilization of small  $Z_x$ 's, it can be directly derived from Eq. (28). Setting Eq. (28) to one single denominator will result in a fraction the numerator of which is a fourth degree polynomial in  $x$ . Therefore,  $T_{33} = 0$  must have four real roots for the system to be stable. We can then reason that (i)  $T_{33}(x)$  is an even function. So, if there are two positive real roots, there will also be two negative real roots and hence a total of four. We can therefore restrict the analysis to  $x > 0$ . (ii) Then,  $\lim_{x \rightarrow +\infty} T_{33}(x) = 1 + \xi > 0$ . (iii) Also,  $\lim_{x \rightarrow \Omega_B/\gamma_0^\pm} T_{33}(x) = \mp \infty$ . (iv) Finally,

$$\lim_{x \rightarrow 0^+} T_{33}(x) = -\text{sgn} \left( \underbrace{\frac{2}{\gamma_0^3} + \frac{Z_x^2}{\beta_0^2} - \frac{2Z_x^2}{\Omega_B^2/\gamma_0}}_{\equiv X} \right).$$

The situation is eventually summarized on Fig. 4. When  $\text{sgn}(X) < 0$ ,  $\lim_{x \rightarrow 0^+} T_{33}(x) = +\infty$  and the equation has but one positive real root. The system is therefore unstable. On the

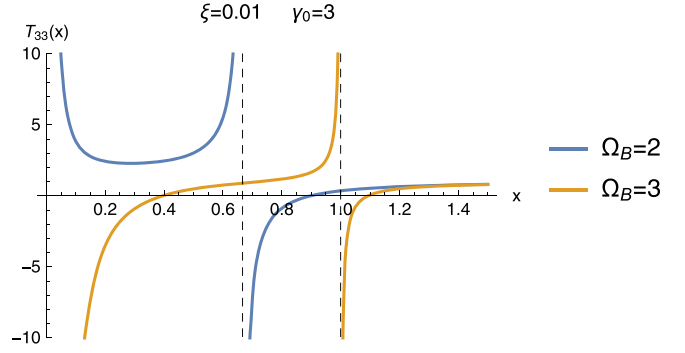


FIG. 4. Plot of  $T_{33}(x)$  given by Eq. (28) for two values of  $\Omega_B$ . For the larger one, the equation  $T_{33}(x) = 0$  has four real roots, whereas it has only two for the smaller  $\Omega_B$ .

contrary, the system is stable with two positive real roots for the equation. The threshold pertains to  $X = 0$ , which exactly gives back Eq. (12).

As previously said, the full dispersion equation for the FI is of the form (26). In the classical case, the factor  $(T_{11}T_{22} - T_{12}^*T_{12})$  does not yield any instability. Here, also, numerical exploration shows that, as long as  $\xi \ll 1$ , this factor does not yield any unstable mode either. We find therefore that QED effects do not affect the smallest unstable  $Z_x$  of the FI nor the saturation value of its growth rate for large  $Z_x$ 's.

Strictly speaking, the FI dispersion equation can be solved exactly since  $T_{33} = 0$ , where  $T_{33}$  is given by Eq. (28), yields a fourth degree polynomial with only even powers. Yet, we understand QED correction for any  $Z_x$  cannot be considerable since the growth rate starts from a point independent of  $\xi$ , and ends up the same way. In this respect, Fig. 5 shows the growth rate of the FI for  $\Omega_B = 1$  and two values of  $\xi$ . A picture similar to the TSI one emerges: QED effects slightly reduce the growth rate.

### C. Oblique instabilities

Surprisingly, what has been found for the TSI and the FI, namely that QED effects reduce the growth rate, is not systematically valid for oblique modes with both  $Z_z \neq 0$  and  $Z_x \neq 0$ . Of course, the two growth rates only slightly differ since  $\xi \ll 1$ , but the forthcoming analysis shows that, in

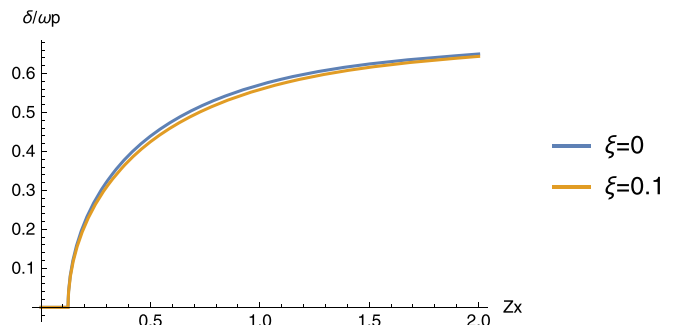


FIG. 5. QED corrected growth rate  $\delta$  of the filamentation instability for  $\Omega_B = 1$  and two values of  $\xi$ .

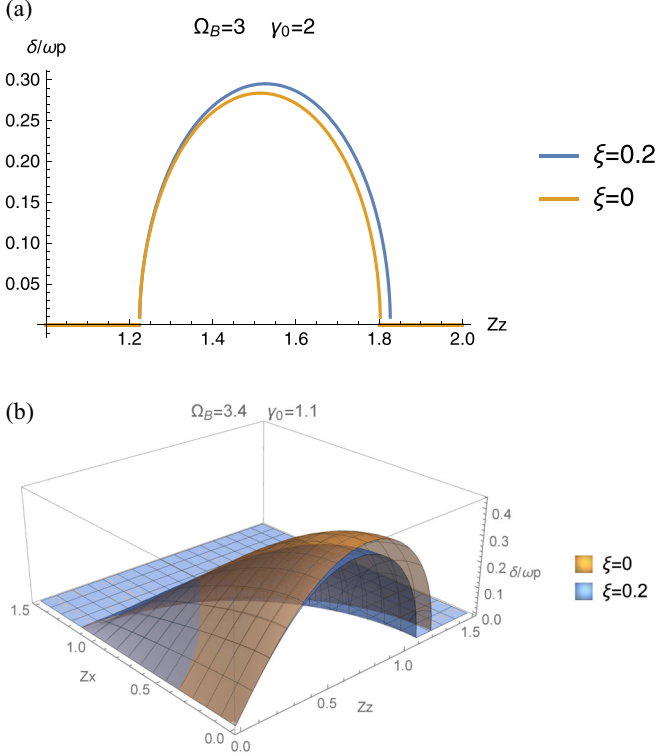


FIG. 6. (a) Growth rate of the oblique modes around  $Z_z = \Omega_B/\gamma_0$  and  $Z_x = \infty$ . The QED corrected growth rate is larger than the classical one. (b) Typical growth rate for the QED ( $\xi = 0.2$ ) and the classical cases when the FI is stabilized with  $\Omega_B > \Omega_{Bc}$ . The value of  $\xi$  is exaggerated in both plots to make QED effects visible.

some regions of the  $\mathbf{k}$  space, the QED corrected growth rate  $\delta_{\text{QED}}$  can be *larger* than the classical one  $\delta_{\text{class}}$ .

We shall first prove analytically that  $\delta_{\text{class}} < \delta_{\text{QED}}$  for some oblique instabilities at large  $k_{\perp}$  (i.e.,  $Z_x \gg 1$ ), before presenting a systematic numerical analysis of the difference.

### 1. Oblique instabilities at $Z_x \gg 1$ and $Z_z = \Omega_B/\gamma_0$

As evidenced on Fig. 3, some oblique unstable modes are found for finite  $Z_z$  and large  $Z_x$ . They were dubbed “upper-

hybrid-like” modes in Ref. [26]. Figure 3 suggests that those found for the lower values of  $Z_z$  vanish at large  $Z_x$ . This will be proved in the forthcoming analysis. Yet, those found at a larger  $Z_z$  persist at  $Z_x \gg 1$ . They are centered around  $Z_z = \Omega_B/\gamma_0$  [26,32], which is a pole of the tensor  $\mathfrak{T}_{\text{class}}$  elements. We can see from Eqs. (20) and (21) that QED corrections do not modify this pole.

An analytical analysis of these unstable modes found at finite  $k_{\parallel}$  (i.e., finite  $Z_z$ ) and large  $k_{\perp}$  ( $Z_x \gg 1$ ) is possible with *Mathematica*. One starts computing the determinant of the tensor  $\mathfrak{T}$  given by Eq. (21). A sum of several rational fractions follows. Setting them all on the same denominator results in a single fraction, the numerator of which is a polynomial  $Q(x, Z_z, Z_x)$ . The dispersion equation reads therefore  $Q(x, Z_z, Z_x) = 0$ .  $Q$  is a polynomial of degree 4 in  $Z_x$ . The dispersion equation for  $Z_x \gg 1$  is therefore the coefficient  $a_4$  of  $Z_x^4$  in  $Q$ . It reads

$$a_4 = \gamma_0^3 (4\xi - 5)(x - Z_z)^2 (x + Z_z)^2 \left( \sum_{j=0}^4 b_j x^j \right), \quad (30)$$

with

$$\begin{aligned} b_0 &= [10\gamma_0 + (5 - 2\xi)\Omega_B^2 + \gamma_0^2(2\xi - 5)Z_z^2] \\ &\quad \times (2\beta_0^2\gamma_0 - \Omega_B^2 + \gamma_0^2Z_z^2), \\ b_1 &= 0, \\ b_2 &= 2\gamma_0^2 \{ \gamma_0 [\beta_0^2(2\xi - 5) + 5] + (5 - 2\xi)\Omega_B^2 \\ &\quad + \gamma_0^2(5 - 2\xi)Z_z^2 \}, \\ b_3 &= 0, \\ b_4 &= \gamma_0^4(2\xi - 5). \end{aligned} \quad (31)$$

The first factor of  $a_4$  does not yield any instability. As for the second one, the QED correction  $\xi \ll 1$  enters its coefficients  $b_j$  in such a way that they will only be slightly modified. And since the roots of a polynomial are continuous functions of its coefficients [33], the associated growth rate is also only slightly modified.

Solving the equation allows one to compute exactly the square of the growth rate. Taylor expanding it for  $\xi \ll 1$  gives

$$\delta = \left[ \delta_{\text{class}}^2 - \frac{2\xi}{5\gamma_0} \left( 1 - \frac{\beta_0^2 + 2\gamma_0 Z_z^2 + 1}{\sqrt{\beta_0^4 + \beta_0^2(2 - 4\gamma_0 Z_z^2) + 4Z_z^2(\gamma_0 + \Omega_B^2) + 1}} \right) + O(\xi^2) \right]^{1/2}. \quad (32)$$

It is interesting to evaluate this expression for  $Z_z = \Omega_B/\gamma_0$ . The result is simply

$$\delta(Z_z = \Omega_B/\gamma_0) = \left[ \delta_{\text{class}}^2 - \frac{2\xi}{5\gamma_0} \left( 1 - \frac{\beta_0^2 + \frac{2\Omega_B^2}{\gamma_0} + 1}{\underbrace{\sqrt{-\frac{4(\beta_0^2 - 1)\Omega_B^2}{\gamma_0} + (\beta_0^2 + 1)^2 + \frac{4\Omega_B^4}{\gamma_0^2}}}_{\equiv A/B}} \right) + O(\xi^2) \right]^{1/2}. \quad (33)$$



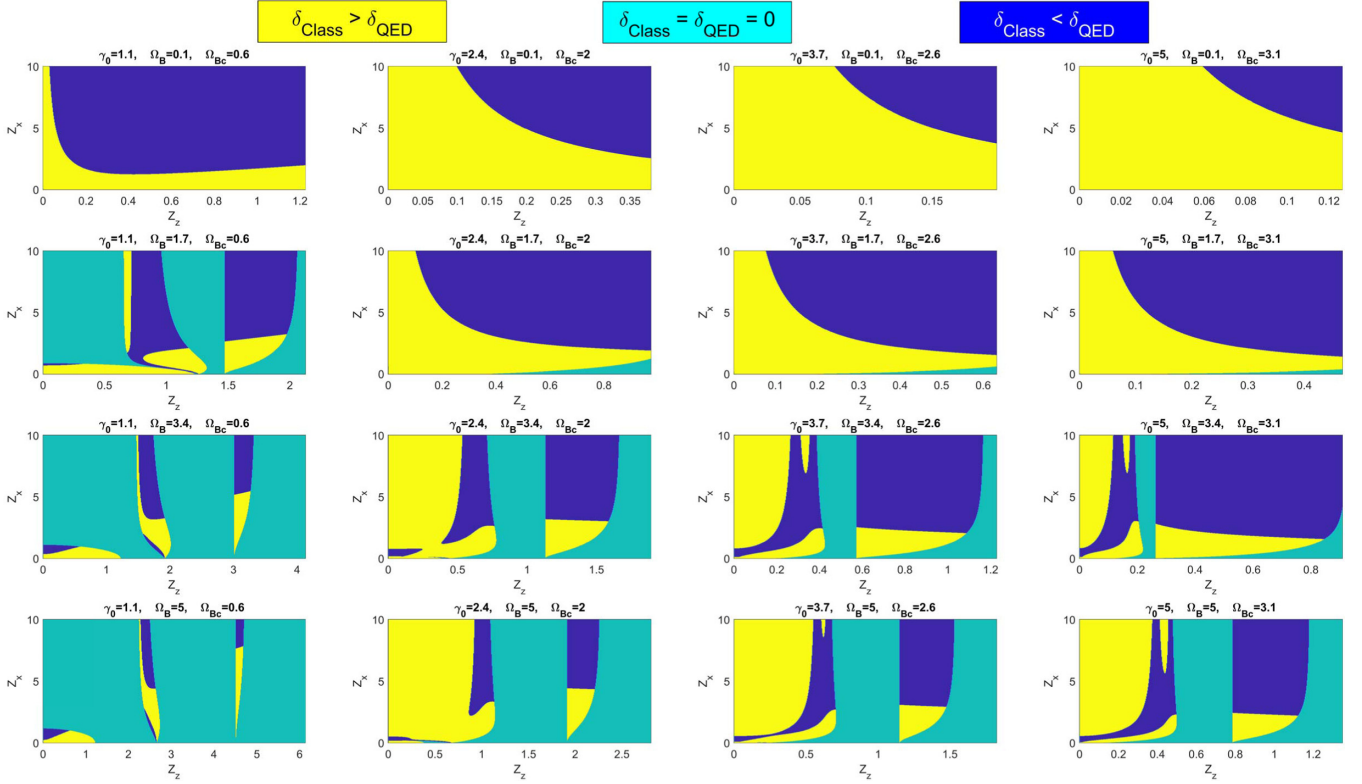


FIG. 7. Plot of  $\delta_{\text{class}} - \delta_{\text{QED}}$  for  $\xi = 10^{-2}$  and various combinations  $(\gamma_0, \Omega_B)$ . The quantity  $\Omega_{Bc}$  indicates the threshold (11) for the stabilization of the FI. While the classical growth rate is larger than the QED one for the TSI and the FI, the contrary can happen for oblique modes (dark blue regions).

Clearly, if  $A/B > 1$ , then the QED growth rate will be *larger* than the classical one, instead of smaller as is the case for the TSI and the FI. Now, some algebra shows that

$$\begin{aligned} B^2 - A^2 &= -\frac{8\beta_0^2\Omega_B^2}{\gamma_0} \\ \Rightarrow \frac{A^2}{B^2} &= 1 + \frac{1}{B^2} \frac{8\beta_0^2\Omega_B^2}{\gamma_0} > 1. \end{aligned} \quad (34)$$

Therefore, for  $Z_z = \Omega_B/\gamma_0$  and  $Z_x \rightarrow \infty$ , the QED corrected growth rate is larger than the classical one. This is illustrated on Fig. 6(a), which shows the two quantities as a function of  $Z_z$ . Note that temperature effects are likely to stabilize these large  $k_\perp$  modes [23,34]. Note also that, since Eq. (30), that is,  $a_4 = 0$ , features only one unstable mode, it means that, out of the two branches visible at large  $Z_x$  on Fig. 3, only one persists in the limit  $Z_x = \infty$ . We just found that this is the one located around  $Z_z = \Omega_B/\gamma_0$ . We now show numerically that  $\delta_{\text{class}} < \delta_{\text{QED}}$  does not occur only at  $Z_z = \Omega_B/\gamma_0$  and  $Z_x \rightarrow \infty$ .

## 2. Numerical study

We now systematically study the difference  $\delta_{\text{class}} - \delta_{\text{QED}}$  over the whole  $\mathbf{k}$  space, for several values of  $\gamma_0$  and  $\Omega_B$ . The result is displayed on Fig. 7. Note that, for faster computation, the polynomial dispersion equation has been transferred from *Mathematica* to *MatLab* using the procedure described in Ref. [35]. For each combination  $(\gamma_0, \Omega_B)$ , the value of

the critical magnetic parameter  $\Omega_{Bc}$  [Eq. (11)] canceling the filamentation instability is indicated on Fig. 7.

These calculations confirm what was previously found. Not only  $\delta_{\text{class}} < \delta_{\text{QED}}$  is fulfilled around  $Z_z = \Omega_B/\gamma_0$  and at large  $Z_x$ 's, but also in several parts of the spectrum. In some cases, the dark blue regions, which indicate places where  $\delta_{\text{class}} < \delta_{\text{QED}}$ , seem to reach the vertical axis  $Z_z = 0$ . One could then think that in such cases we have  $\delta_{\text{class}} < \delta_{\text{QED}}$  for the FI, in contradiction with the conclusions of Sec. III B.

Yet, as shown for example on Fig. 6(b), this is not the case. On this plot, the FI is stabilized since  $\Omega_B = 3.4 > \Omega_{Bc} = 0.6$ . While we retrieve  $\delta_{\text{class}} > \delta_{\text{QED}}$  for the TSI, there is a region near  $0.5 \lesssim Z_x \lesssim 1$  where  $\delta_{\text{class}} < \delta_{\text{QED}}$ , while both go to zero simultaneously for  $Z_z = 0$  since the criteria for canceling them is the same. In other words, we do not find here  $\delta_{\text{class}}(Z_x = 0) < \delta_{\text{QED}}(Z_x = 0)$ . Instead, we find cases with  $\delta_{\text{class}}(Z_x = 0^+) > \delta_{\text{QED}}(Z_x = 0^+)$  and  $\delta_{\text{class}}(Z_x = 0) = \delta_{\text{QED}}(Z_x = 0) = 0$ .

## IV. CONCLUSION

We computed the QED corrections to counter-streaming instabilities resulting from harmonic perturbations with any possible orientation of the wave vector. As was the case for the TSI, finite first order corrections demand the presence of a flow-aligned static magnetic field  $\mathbf{B}_0$ . If  $B_0 = 0$ , the fields cannot reach high enough intensities when growing from zero during the linear phase for QED effects to appear.

Note that QED effects could arise during the *nonlinear* phase of an *unmagnetized* system if the field at saturation approaches the Schwinger limit  $B_{cr}$ . For example, the saturation value  $B_{sat}$  of the magnetic field for the filamentation instability is of the order of [36,37]

$$B_{sat} = \sqrt{\gamma_0} \frac{mc\omega_p}{q}, \quad (35)$$

so that  $B_{sat} \sim B_{cr}$  gives

$$\begin{aligned} \sqrt{\gamma_0} \frac{mc\omega_p}{q} &\sim \frac{m^2 c^3}{q\hbar} \Rightarrow \gamma_0 \sim \frac{1}{\omega_p^2} \frac{m^2 c^4}{\hbar^2} \\ &\Rightarrow \gamma_0 \sim \left(\frac{\ell_e}{\ell_C}\right)^2, \end{aligned} \quad (36)$$

where  $\ell_e = c/\omega_p$  is the electron inertial length and  $\ell_C = \hbar/mc$  the reduced electronic Compton wavelength. With  $\ell_C = 3.8 \times 10^{-11}$  cm and  $\ell_e = 5.3 \times 10^5 n_e^{-1/2}$  cm, where  $n_e$  is the electronic density in  $\text{cm}^{-3}$  [38], this translates to

$$\gamma_0 \sim \frac{1.9 \times 10^{32}}{n_e [\text{cm}^{-3}]}. \quad (37)$$

Hence  $B_{sat} \sim B_{cr}$  could be achieved for extremely high Lorentz factors and/or beam densities.

Previous results for the TSI are recovered. In addition, we find here that, even in 3D, the QED corrected TSI remains a 1D problem.

Choosing the wave vector perpendicular to the flow allows one to analyze the FI. We find that QED effects neither change the smallest unstable  $k_{\perp}$  nor the growth rate at large  $k_{\perp}$ . In between, QED corrections slightly decrease the growth rate.

Noteworthy, when it comes to oblique unstable modes, analytical and numerical calculations do *not* confirm the trends found for the TSI and the FI. While the growth rate reductions can be attributed to virtual particles screening the charges (see [31], p. 482), its increase in some regions of the  $\mathbf{k}$  space is surprising.

Some important effects have been left out of this article. When particles oscillate in the first order growing fields, they may emit  $\gamma$  photons, which in turn trigger pair production [39,40]. These effects should arguably be worked out in future works.

#### ACKNOWLEDGMENTS

A.B. acknowledges support by Grants No. ENE2016-75703-R from the Spanish Ministerio de Ciencia, Innovación y Universidades and No. SBPLY/17/180501/000264 from the Junta de Comunidades de Castilla-La Mancha. Thanks are due to L. Silva and T. Grismayer for valuable input.

- 
- [1] I. Langmuir, Scattering of electrons in ionized gases, *Phys. Rev.* **26**, 585 (1925).
  - [2] J. R. Pierce, Possible fluctuations in electron streams due to ions, *J. Appl. Phys.* **19**, 231 (1948).
  - [3] D. A. Uzdensky and S. Rightley, Plasma physics of extreme astrophysical environments, *Rep. Prog. Phys.* **77**, 036902 (2014).
  - [4] L. O. Silva, Extreme plasma physics, Plenary Talk at the 47th EPS Conference on Plasma Physics, 2021 (unpublished).
  - [5] C. Danson, D. Hillier, N. Hopps, and D. Neely, Petawatt class lasers worldwide, *High Power Laser Sci., Eng.* **3**, e3 (2015).
  - [6] B. King and T. Heinzl, Measuring vacuum polarization with high-power lasers, *High Power Laser Sci., Eng.* **4**, e5 (2016).
  - [7] D. Lai, Physics in very strong magnetic fields, *Space Sci. Rev.* **191**, 13 (2015).
  - [8] K. Qu, S. Meuren, and N. J. Fisch, Collective plasma effects of electron-positron pairs in beam-driven QED cascades, [arXiv:2110.12592](https://arxiv.org/abs/2110.12592).
  - [9] A. M. Beloborodov and C. Thompson, Corona of magnetars, *Astrophys. J.* **657**, 967 (2007).
  - [10] M. Gedalin, E. Gruman, and D. B. Melrose, New Mechanism of Pulsar Radio Emission, *Phys. Rev. Lett.* **88**, 121101 (2002).
  - [11] E. Asseo, Pair plasma in pulsar magnetospheres, *Plasma Phys. Controlled Fusion* **45**, 853 (2003).
  - [12] D. B. Melrose, Coherent emission mechanisms in astrophysical plasmas, *Rev. Mod. Plasma Phys.* **1**, 5 (2017).
  - [13] V. V. Usov, Millisecond pulsars with extremely strong magnetic fields as a cosmological source of  $\gamma$ -ray bursts, *Nature (London)* **357**, 472 (1992).
  - [14] N. Bucciantini, E. Quataert, J. Arons, B. D. Metzger, and T. A. Thompson, Relativistic jets, and long-duration gamma-ray bursts from the birth of magnetars, *Mon. Not. R. Astron. Soc.* **383**, L25 (2008).
  - [15] B. D. Metzger, D. Giannios, T. A. Thompson, N. Bucciantini, and E. Quataert, The protomagnetar model for gamma-ray bursts, *Mon. Not. R. Astron. Soc.* **413**, 2031 (2011).
  - [16] A. Bret, Quantum electrodynamic effects on the two-stream instability, *Europhys. Lett.* **135**, 35001 (2021).
  - [17] K. M. Watson, S. A. Bludman, and M. N. Rosenbluth, Statistical Mechanics of Relativistic Streams. I, *Phys. Fluids* **3**, 741 (1960).
  - [18] S. A. Bludman, K. M. Watson, and M. N. Rosenbluth, Statistical mechanics of relativistic streams. II, *Phys. Fluids* **3**, 747 (1960).
  - [19] Y. B. Faïnberg, V. D. Shapiro, and V. I. Shevchenko, Nonlinear theory of interaction between a “monochromatic” beam of relativistic electrons, and a plasma, *Zh. Eksp. Teor. Fiz.* **57**, 966 (1969) [*Sov. Phys. JETP* **30**, 528 (1970)].
  - [20] A. Bret and C. Deutsch, Hierarchy of beam plasma instabilities up to high beam densities for fast ignition scenario, *Phys. Plasmas* **12**, 082704 (2005).
  - [21] A. Bret, L. Gremillet, D. Bénisti, and E. Lefebvre, Exact Relativistic Kinetic Theory of An Electron-Beam-Plasma System: Hierarchy of the Competing Modes in the System-Parameter Space, *Phys. Rev. Lett.* **100**, 205008 (2008).
  - [22] A. Bret, Weibel, two-stream, filamentation, oblique, bell, buneman...which one grows faster? *Astrophys. J.* **699**, 990 (2009).
  - [23] A. Bret, L. Gremillet, and M. E. Dieckmann, Multidimensional electron beam-plasma instabilities in the relativistic regime, *Phys. Plasmas* **17**, 120501 (2010).

- [24] A. Bret, Hierarchy of instabilities for two counter-streaming magnetized pair beams, *Phys. Plasmas* **23**, 062122 (2016).
- [25] A. Bret and M. E. Dieckmann, Hierarchy of instabilities for two counter-streaming magnetized pair beams: Influence of field obliquity, *Phys. Plasmas* **24**, 062105 (2017).
- [26] B. B. Godfrey, W. R. Shanahan, and L. E. Thode, Linear theory of a cold relativistic beam propagating along an external magnetic field, *Phys. Fluids* **18**, 346 (1975).
- [27] A. Bret, *Comput. Phys. Commun.* **176**, 362 (2007).
- [28] See Supplemental Material at <http://link.aps.org/supplemental/10.1103/PhysRevE.105.015205> for Mathematica Notebook used to compute the dispersion equation.
- [29] A. Di Piazza, K. Z. Hatsagortsyan, and C. H. Keitel, Enhancement of vacuum polarization effects in a plasma, *Phys. Plasmas* **14**, 032102 (2007).
- [30] A. Di Piazza, C. Müller, K. Z. Hatsagortsyan, and C. H. Keitel, Extremely high-intensity laser interactions with fundamental quantum systems, *Rev. Mod. Phys.* **84**, 1177 (2012).
- [31] S. Weinberg, *The Quantum Theory of Fields: Volume 1, Foundations* (Cambridge University Press, Cambridge, UK, 2005).
- [32] A. Bret, M. Dieckmann, and C. Deutsch, Oblique electromagnetic instabilities for a hot relativistic beam interacting with a hot and magnetized plasma, *Phys. Plasmas* **13**, 082109 (2006).
- [33] D. J. Uherka and A. M. Sergott, On the continuous dependence of the roots of a polynomial on its coefficients, *Am. Math. Mon.* **84**, 368 (1977).
- [34] L. O. Silva, R. A. Fonseca, J. W. Tonge, W. B. Mori, and J. M. Dawson, On the role of the purely transverse Weibel instability in fast ignitor scenarios, *Phys. Plasmas* **9**, 2458 (2002).
- [35] A. Bret, Transferring a symbolic polynomial expression from Mathematica to Matlab, [arXiv:1002.4725](https://arxiv.org/abs/1002.4725).
- [36] R. C. Davidson, D. A. Hammer, I. Haber, and C. E. Wagner, Nonlinear development of electromagnetic instabilities in anisotropic plasmas, *Phys. Fluids* **15**, 317 (1972).
- [37] A. Bret, A. Stockem, F. Fiuza, C. Ruyer, L. Gremillet, R. Narayan, and L. O. Silva, Collisionless shock formation, spontaneous electromagnetic fluctuations, and streaming instabilities, *Phys. Plasmas* **20**, 042102 (2013).
- [38] D. L. Book, NRL plasma formulary, 2019.
- [39] T. Grismayer, M. Vranic, J. L. Martins, R. A. Fonseca, and L. O. Silva, Laser absorption via quantum electrodynamics cascades in counter propagating laser pulses, *Phys. Plasmas* **23**, 056706 (2016).
- [40] T. Grismayer, M. Vranic, J. L. Martins, R. A. Fonseca, and L. O. Silva, Seeded QED cascades in counterpropagating laser pulses, *Phys. Rev. E* **95**, 023210 (2017).